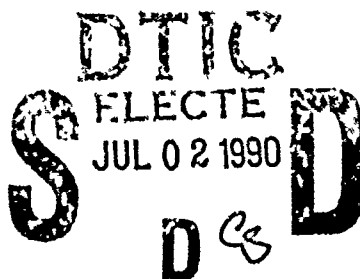RADC-TR-90-87
In-House Report
May 1990

RELIABILITY STUDY OF TWT OUTPUT RF WINDOW

AD-A223 688
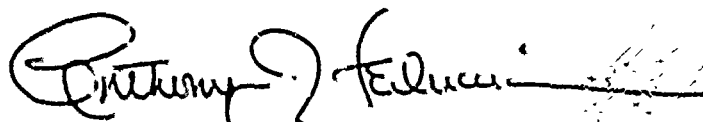
Peter J. Rocci

DTIC
ELECTE
JUL 0 2 1990
S D

Rome Air Development Center
Air Force Systems Command
Griffiss Air Force Base, NY 13441-5700

DTIC 06 29 003

This report has been reviewed by the RADC Public Affairs Division (PA) and is releasable to the National Technical Information Service (NTIS). At NTIS it will be releasable to the general public, including foreign nations.
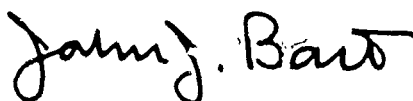
RADC-TR-90-87 has been reviewed and is approved for publication.
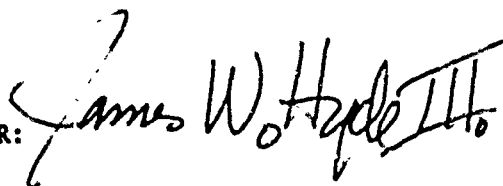
APPROVED:

ANTHONY J. FEDUCCIA, Chief
Systems Reliability & Engineering Division
Directorate of Reliability & Compatibility

APPROVED:

JOHN J. BART
Technical Director
Directorate of Reliability & Compatibility

FOR THE COMMANDER:

JAMES W. HYDE III
Directorate of Plans & Programs

REPORT DOCUMENTATION PAGE

Public reporting burden for this collection of information is estimated to average 1 hour per response, including the time for reviewing instructions, searching existing data sources, gathering and maintaining the data needed, and reviewing the collection of information. Send comments regarding this burden estimate or any other aspect of this collection of information, including suggestions for reducing this burden, to Washington Headquarters Services, Directorate for Information Operations and Reports, 1215 Jefferson Davis Highway, Suite 1204, Arlington, VA 22202-4302, and to the Office of Information and Regulatory Affairs, Office of Management and Budget, Washington, DC 20503.

1 AGENCY USE ONLY (Leave Blank)	2. REPORT DATE	3 REPORT TYPE AND DATES COVERED
	May 1990	In-House Feb 89 – Oct 89

4 TITLE AND SUBTITLE	5 FUNDING NUMBERS
RELIABILITY STUDY OF TWT OUTPUT RF WINDOW	PE – 62702F
	PR – 2338
6 AUTHOR(S)	TA – 02
	WU – 2P
Peter J. Rocci	

7 PERFORMING ORGANIZATION NAME(S) AND ADDRESS(ES)	8 PERFORMING ORGANIZATION REPORT NUMBER
Rome Air Development Center (RBES) Griffiss AFB NY 13441-5700	RADC-TR-90-87

9 SPONSORING/MONITORING AGENCY NAME(S) AND ADDRESS(ES)	10 SPONSORING/MONITORING AGENCY REPORT NUMBER
Rome Air Development Center (RBES) Griffiss AFB NY 13441-5700	N/A

11 SUPPLEMENTARY NOTES

RADC Project Engineer: Peter J. Rocci/RBES/(315) 330-4891

12a. DISTRIBUTION/AVAILABILITY STATEMENT	12b. DISTRIBUTION CODE
Approved for public release; distribution unlimited. →Rome Air Development Center	(nickel-copper)

13 ABSTRACT (Maximum 200 words)

RADC's Computer-Aided Systems Engineering Branch, RBES, has documented an in-house effort to evaluate the structural reliability of the output waveguide window on a Traveling Wave Tube (TWT). This window acts as a seal between the TWT's vacuum envelope and output waveguide. Its purpose is to prevent any loss due to leakage of the vacuum while allowing passage of the microwave signal. This particular disk-shaped window is constructed of a ceramic material, beryllia, and contains an inner ring of copper and an outer ring of Mon 1 K-500 (70-30 Ni-Cu). It was suspected that excessive thermal stresses associated with the very high operating temperatures by this window had caused it to fail.

Finite element analyses, along with material failure theories were used to determine the window's response to a time-dependent heat source and operating heat sink temperature. Analyses were made for various rates of heat dissipation through the window ranging from 20 to 120 watts. It was determined that cracking of the

14 SUBJECT TERMS	15 NUMBER OF PAGES
Traveling Wave Tube, Finite Element Method, Thermal Stress, TWT, Electrical and Electronic Equipment, Ceramic Material, Beryllia	60
	16 PRICE CODE

17 SECURITY CLASSIFICATION OF REPORT	18 SECURITY CLASSIFICATION OF THIS PAGE	19 SECURITY CLASSIFICATION OF ABSTRACT	20 LIMITATION OF ABSTRACT
UNCLASSIFIED	UNCLASSIFIED	UNCLASSIFIED	UL

NSN 7540-01-280-5500

Standard Form 298 (Rev. 2-89)
Prescribed by ANSI Std. Z39-18
298-101

(3G)

beryllia at its outer edge could occur if more than 20 watts of heat were to be dissipated through the window. The effect of power cycling on the window's ductile materials (copper and Monel) was also studied. It was found that, depending on the amount of heat dissipation, the copper portion of the window could survive between 500 and 9000 power cycles before failure would occur.

PREFACE

The structural reliability of a ceramic RF output window of a Traveling Wave Tube (TWT) is assessed in this report. This TWT was part of the ALQ-99 ECM system currently in service on the EF-111 aircraft. The Finite Element program, Numerically Integrated Elements For Systems Analysis (NISA), along with material failure theories were utilized for this analysis. All of the work was accomplished in-house at RADC.

The author wishes to thank Mr. Edward J. Jones, Ms. Gretchen A. Bivens, Mr. Douglas J. Holzhauer, and Mr. William Bocchi, RADC/RBES, along with Dr. Edward Daniszewski, RADC/OCTP, for their technical assistance on this project.

Accesion For		
NTIS CRA&I		V
DTIC TAB		☐
Unannounced		☐
Justification		
By		
Distribution /		
Availability Codes		
Dist	Avail and/or Special	
A-1		

i

TABLE OF CONTENTS

ILLUSTRATIONS

0.0 EXECUTIVE SUMMARY

The objective of this study was to investigate the physical integrity of a TWT's output RF window (Figure 1). This window is part of a TWT that is used in the ALQ-99 ECM system. The output energy that this window is subject to causes the window to experience very high operating temperatures that cause high material stresses which adversely affect its reliability. The window analyzed in this study had been taken from a failed TWT and was found to be cracked. Many microwave tube failures have been attributed to mechanical stresses induced in the output window by heat sources which induce a temperature distribution throughout the window. Any quantitative analysis of this phenomena involves the calculation of temperature and stress distributions. Heating conditions that caused cracking of the window and also the effects of power cycling on the system (number of power cycles to failure) were determined. These are good indications of the window's design reliability.

In order to assess the window's reliability, finite element simulations were employed. Finite Element Analysis (FEA) is a computer simulation technique which predicts the physical behavior of a system under any specified type(s) of load(s). A geometric model of the system is generated and the material properties of the model are defined within the input data file. The data file also contains thermal loads and/or physical constraints on the system (depending on the type of analysis being performed). The data file is then read by the finite element code and the analysis is
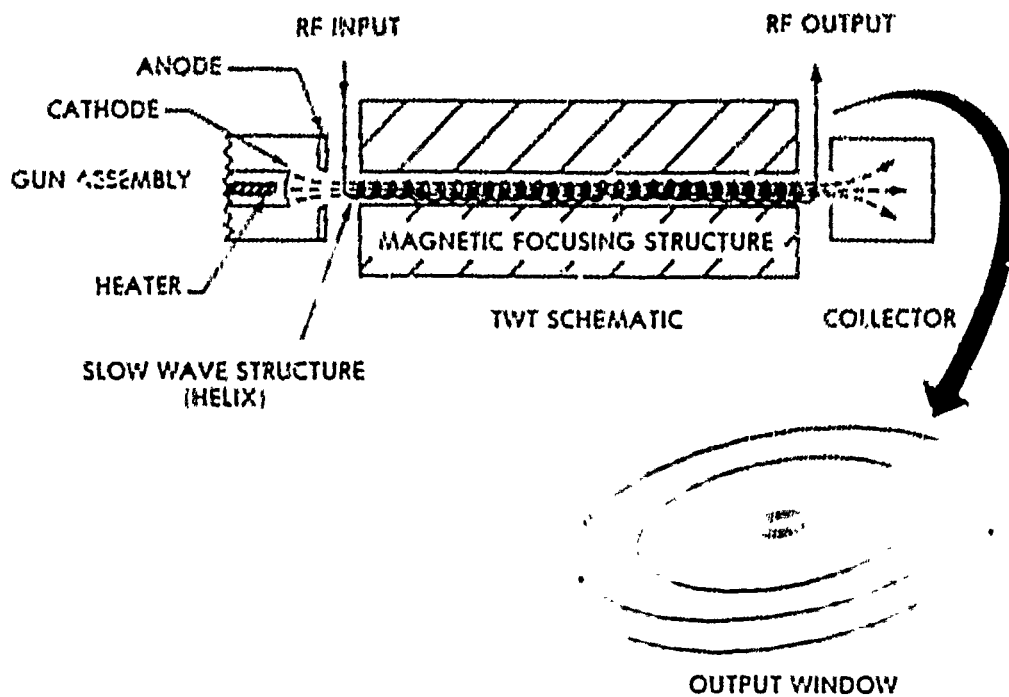
RF Window Location
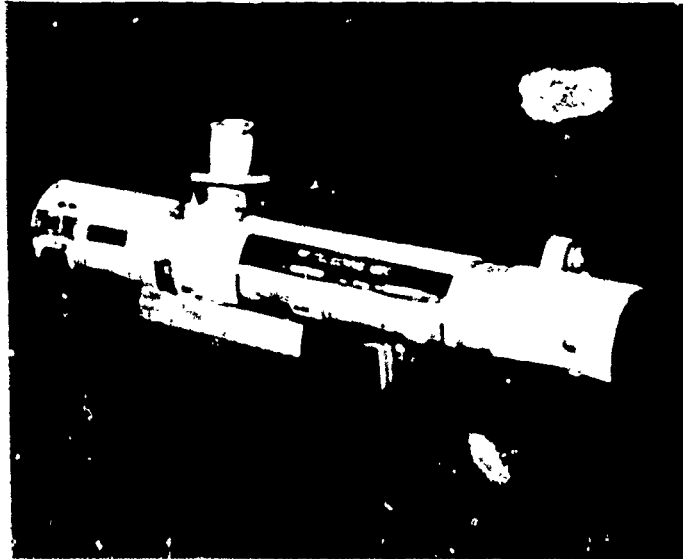
TRAVELING WAVE TUBE

FIGURE 1

2

performed. Several parametric studies were made of this window using this technique and the results used to assess the window's reliability.

The results of the parametric studies made by finite element analyses were used in conjunction with the Manson-Coffin equation to predict the number of power cycles the copper portion of the window would survive in the ALQ-99 environment. The Manson-Coffin equation is an empirical relation based on fatigue-life data which considers the total strain within a ductile material and the effect of load reversals on these strains. One power cycle was considered to represent one loading cycle. Therefore, the number of power cycles to failure indicates how many times the TWT can be operated before window failure would occur.

A plot was obtained relating heat dissipation through the window to power cycles to failure. From this plot, for any value of heat dissipation rate (ranging from 20 to 120 watts) the number of power cycles to failure could be determined for the copper portion of the window. Within this heating range, the number of power cycles to failure was found to vary from 500 to 9000 cycles. FEA results were also used in conjunction with the maximum normal stress theory for brittle fracture to determine what conditions would cause the beryllia portion of the window to crack. It was determined that for heat dissipation rates through the window of greater than 20 watts, the beryllia would begin to crack at its outer circumference.

All conclusions were made on the assumption that there were no manu-
facturing defects associated with the window. Failure could only be caused
by design defects or tube operation beyond design capabilities. Struc-
tural failure is but one failure mode associated with TWT's. A study is
currently underway at RADC to identify other failure modes associated with
TWT's. It is anticipated that the results of these studies will provide
information that would lead to design and manufacturing of more reliable
Traveling Wave Tubes.

1.0 INTRODUCTION

A Traveling Wave Tube (TWT) is an electron tube used for amplification of microwave and millimeter wave signals. Its operation depends on the interaction of a beam of electrons with an electromagnetic wave. Some applications of TWT's include use in space communications, electronic warfare, radar and the relaying of home video signals.

Investigation of the effect of high operating temperatures on the structural reliability of a TWT's output window was the main objective of this study. If temperature limits are exceeded due to high heat dissipation and/or inadequate cooling methods, the resulting thermal stresses can reach a high enough value to cause cracking or fatigue failure of the window.

The most widely used waveguide window for high-power tubes is the circular ceramic disk window in a section of round waveguide. This type of window can achieve a bandwidth in the thirty percent range and has a high average and peak power handling capability (8). This ceramic window is constructed of beryllia (BeO). Beryllia ceramic windows are used for high average power outputs because of their good thermal conductivity at high temperatures (111 W/M-C at 325°C or 64.14 BTU/hr-ft-F at 600°F). Beryllia is avoided in many cases for window applications because of its toxicity, unless its high thermal conductivity is an absolute requirement. The material is used more as an electrical insulator where the chance of exposure to beryllia in powder form is very slim (8).

5

The system analyzed in this study and its dimensions are shown in Figure 2. This system consists of the beryllia disk which surrounds a thin-walled copper tube through which the output RF energy is conducted. The beryllia disk is surrounded by a nickel-copper alloy. A laboratory analysis determined the composition of this alloy to be 64% nickel and 36% copper. This material was assigned the properties of Monel K-500 (70-30 Ni-Cu), the material whose composition most closely resembled the alloy's composition.

When the TWT is powered up, current flow through the copper interacts with the copper atoms causing displacement and heat generation. The system experiences a uniform temperature distribution which induces a thermal stress distribution throughout the disk. If these stresses reach a high enough value, the beryllia disk, which behaves in a brittle manner, can be expected to crack.

The effect of thermal cycling from repeatedly powering up and powering down the system can lead to fatigue failure of the window. When the system is powered up, the ductile materials in the window (copper and monel) become strained due to thermal stresses. After the system is powered down, the materials return to their original thermal state. However, not all of the total strain is recovered. A portion remains within the material due to plastic deformation. Every time this process is repeated, strain accumulates within the material and after a certain number of power cycles, the total strain within the material can reach a

6

TWT Output RF Window
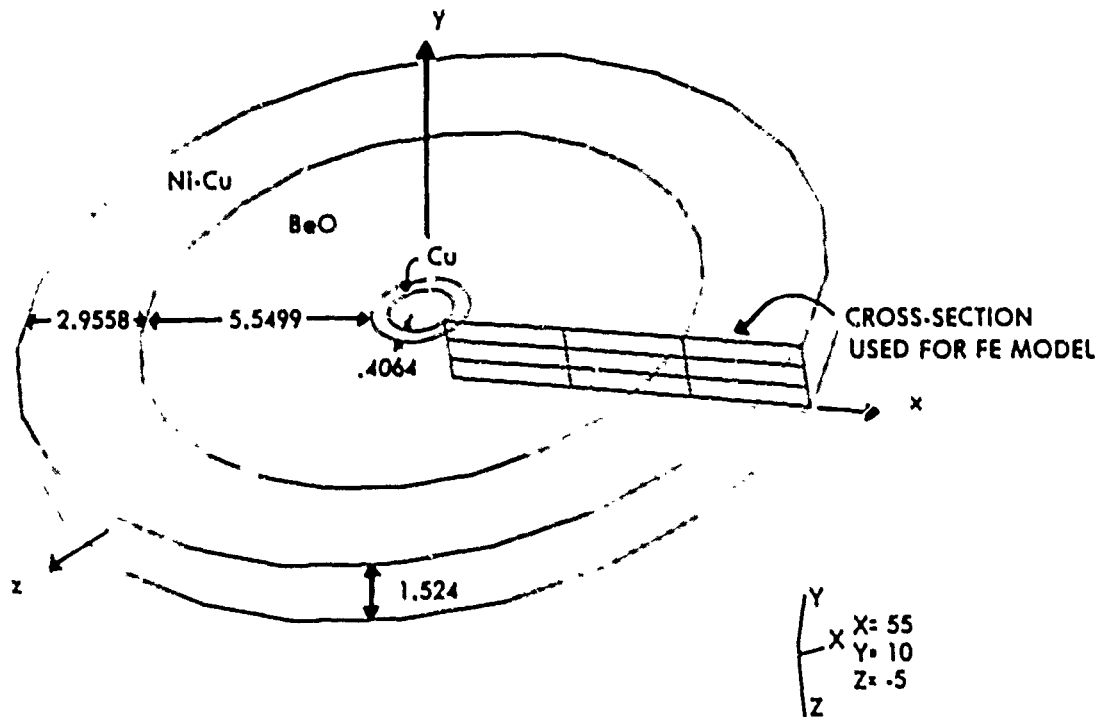
NOTE: ALL DIMENSIONS IN MILLIMETERS

FIGURE   2

great enough value to cause failure. The predicted number of power cycles to failure gives a good indication of the window's reliability.

MIL-HDBK-217, Reliability Prediction of Military Equipmen , "ides a model to predict the operating failure rate for Traveling Wave Tubes based on tube characteristics and operating environment. This model was formulated from failure data obtained from previously designed tubes and only considers the reliability of the overall TWT. Since no mathematical model exists that can be used to predict the reliability of an output window, an alternate method is needed. Therefore, several parametric studies were made of the window using finite element techniques and the results used to assess the window's reliability. Research into this area turned up no reports of previous finite element analyses done on TWT output windows.

The FEA code used at RADC is Numerically Integrated Elements for System Analysis (NISA). In this study, NISA's transient heat transfer code was used to simulate the system's response to a heat input and time varying operating heat sink temperature. The resulting temperature distribution was used as a thermal load into NISA's nonlinear static stress module. Nonlinear stress analyses were performed to account for the plastic behavior experienced by the ductile materials of the system beyond their respective yield points. Stresses beyond a material's yield point will cause the material to deform in a plastic manner. Results from the nonlinear analyses were used in the maximum normal stress formula to predict

8

a heating value that would cause brittle failure of the beryllia to occur. These results were also used in the Manson-Coffin equation in order to predict a number of power cycles to failure for the copper portion of the window.

This report is organized in the following manner. First, a des⸴ ⸴p-tion of the finite element model is given. Second, the inputs i⸴to ⸴he transient heat transfer code are described along with the resulting temperature distributions for different heating values. These results are then input to the nonlinear code which gives the resulting stress distributions throughout the window. Finally, results from the stress analyses are interpreted using material failure theories for both brittle and ductile materials.

2.0 FINITE ELEMENT MODEL

Finite element models are geometric models that represent an actual physical system. Since heat was being generated on the entire inner diameter of the copper, the heat transfer was axisymmetric; that is, the temperature varied only in the radial direction (x-direction) (Figure 2). Because the window is of uniform thickness, it was also assumed that the temperature remained constant throughout the thickness of the disk (y-direction). With these assumptions, the heat transfer is actually one-dimensional, however, to better visualize the temperature distribution throughout the system, a two-dimensional model was created. The geometric model is illustrated in Figure 3. Figure 3 is oriented such that the x-axis represents the radial direction and the y axis represents the axis of rotation. This model is a two-dimensional cross-section of Figure 2 taken parallel to the x-y plane (looking into the z axis).

Using NISA's Geometry Data Base Computer Program, this model was easily created. The model was divided into four patches (regions) with each patch representing a different material. Patch 1 represents a very elastic material used to simulate boundary conditions. This patch was assigned highly elastic properties and its purpose was to represent the space between the y-axis and the copper (patch 2). The space was represented in this way so that the model could be properly constrained in the x and y directions. Constraining the left-hand side of the copper would have been invalid since the whole model must be allowed to expand radially.
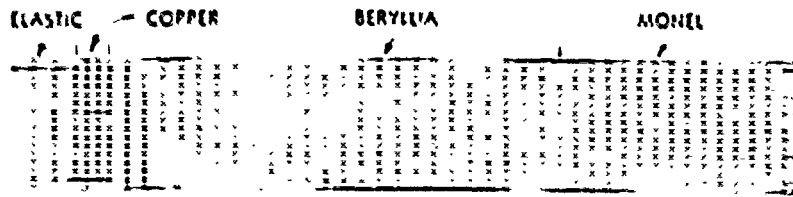
Geometric Model
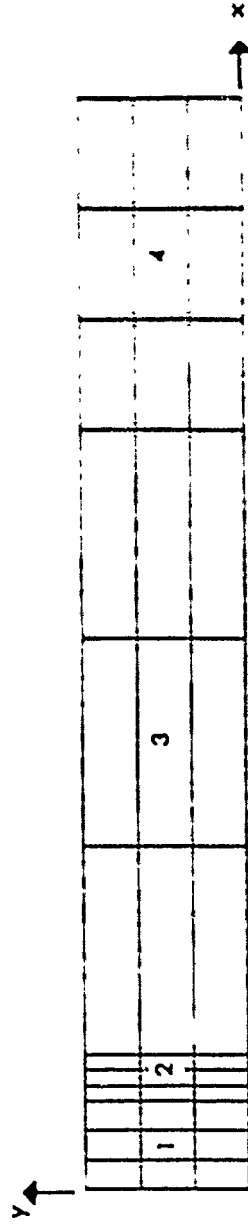
Cross-Section From Figure 2

FIGURE 3

11

Patches 4 and 9 were assigned the properties of beryllia and Monel K-500, respectively.
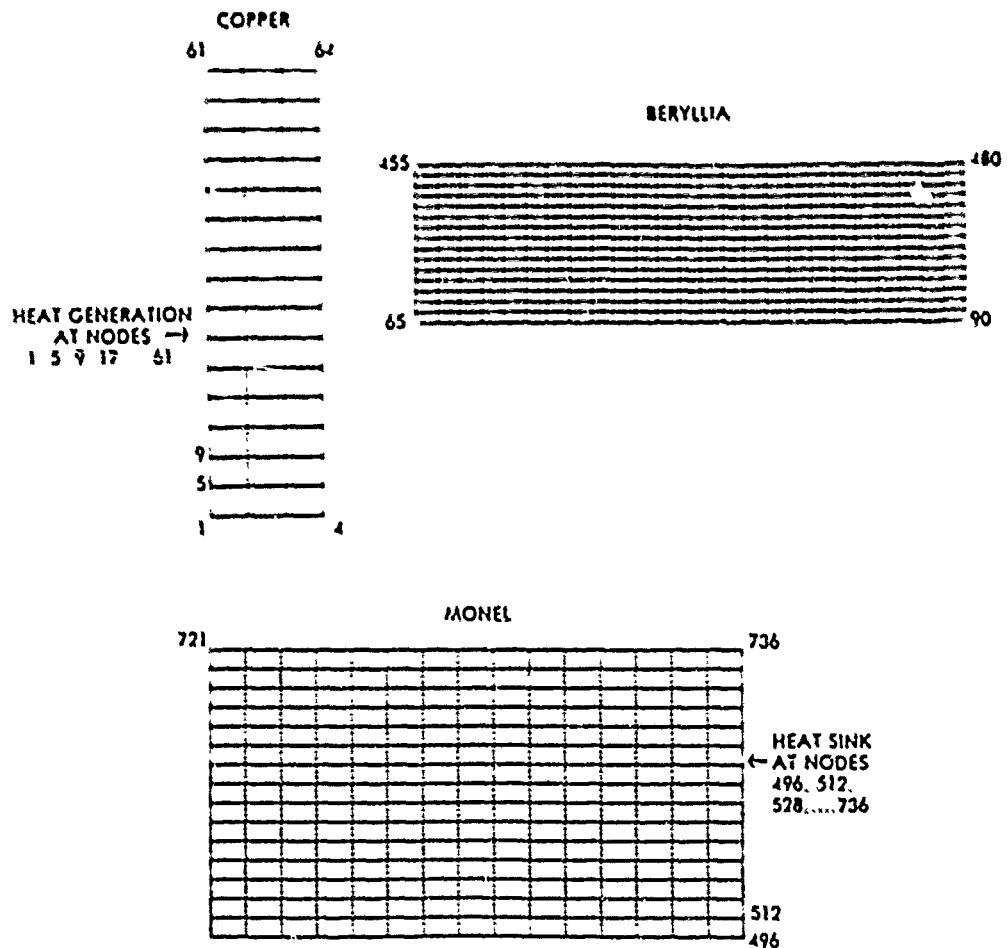
The finite element model (Figure 4) is defined by two mathematical parameters, nodes and elements. A node is a grid point located in space. Since this model was created in two dimensions, each node was defined by two coordinates, x and y. The element is defined by a material index number and a set of nodes. Each index number has specific material properties associated with it. The properties can be defined to be constant or temperature dependent. Two of the materials, copper and beryllia, had temperature-dependent thermal conductivities. A few sets of data points were input into the data file and the NISA code linearly interpolated between these points to determine the conductivity at any temperature. Only one value of thermal conductivity could be found for monel, therefore, its thermal conductivity was assumed to be independent of temperature. Since the thermal conductivities of most metals do not depend heavily on temperature, this is a reasonable assumption.

The elements used in this study were two-dimensional, four-sided, axisymmetric solid elements. Each element was defined by four nodes, one at each corner. Two types of these elements were utilized, the first for the heat transfer analysis and the second for the nonlinear static stress analysis. These elements were identical in shape and orientation with their only difference being that the heat transfer element has only one degree of freedom, temperature, while the static element has two degrees of freedom, movement in both the x and y directions.

12

Finite Element Model

Entire Axisymmetric Model

Regions That Represent The Materials Of The Model

FIGURE 4

The finite element model contains a total of 800 nodes and 690 elements. Each material contains the following node and element numbers:

Material	Node #'s	Element #'s
Copper	1-64	1-45
Beryllia	65-480	46-420
Monel	481-736	421-645
Elastic	737-800	646-690

The results obtained for the elastic material were reviewed to verify the accuracy of this technique, but not considered in the stress analyses.

For both heat transfer and static stress analyses, all nodes lying on a boundary between materials were coupled to each other. What this means is that for the thermal analyses, these nodes were required to have the same temperature and for the stress analyses, they were required to move equal amounts in both the x and y directions. If these nodes were merged instead of coupled, the temperature and stress results given would have been average values between nodes of two dissimilar materials, which would have been inaccurate. If these nodes were left uncoupled, the NISA programs would not execute due to disjointed elements at the boundaries.

3.0 TRANSIENT HEAT TRANSFER ANALYSIS

Model

A transient heat transfer analysis simulates the model's thermal state when the temperature distribution varies with time. Since the window is enclosed in a section of round waveguide, it was assumed that the primary mode of heat transfer was conduction. There was no convection or radiation to the outside air. The thermal resistance associated with conduction is considerably less than the resistances for convection and radiation, therefore, this is a reasonable assumption. This case of pure conduction represents a worse case scenario under which the window's reliability will be characterized.

This analysis was performed with heat being generated on the entire inner diameter of the copper. The heat generation was simulated as concentrated nodal heat fluxes at nodes 1, 5, 9, 13, 17, 21, 29, 33, 37, 41, 45, 53 and 61 (see Figure 4). In order to provide a path for the heat to flow, a heat sink temperature was designated at the outer edge of the monel. These nodes represent the extreme outer edge of the model (see Figure 4). The heat sink represents an area where the system is cooled to a specified temperature to prevent possible melting of any components. A tube operating temperature profile was measured during an actual ALQ-99 mission flight test of the tube and is shown in the curve of Figure 5. This data was obtained from temperature readings taken on the top of TWT's beam collector. The location of the collector is close to the outer edge of the

15

ALQ-99 Environmental Flight Test Profile

TUT BEAM COLLECTOR TEMPERATURE (DEG C)

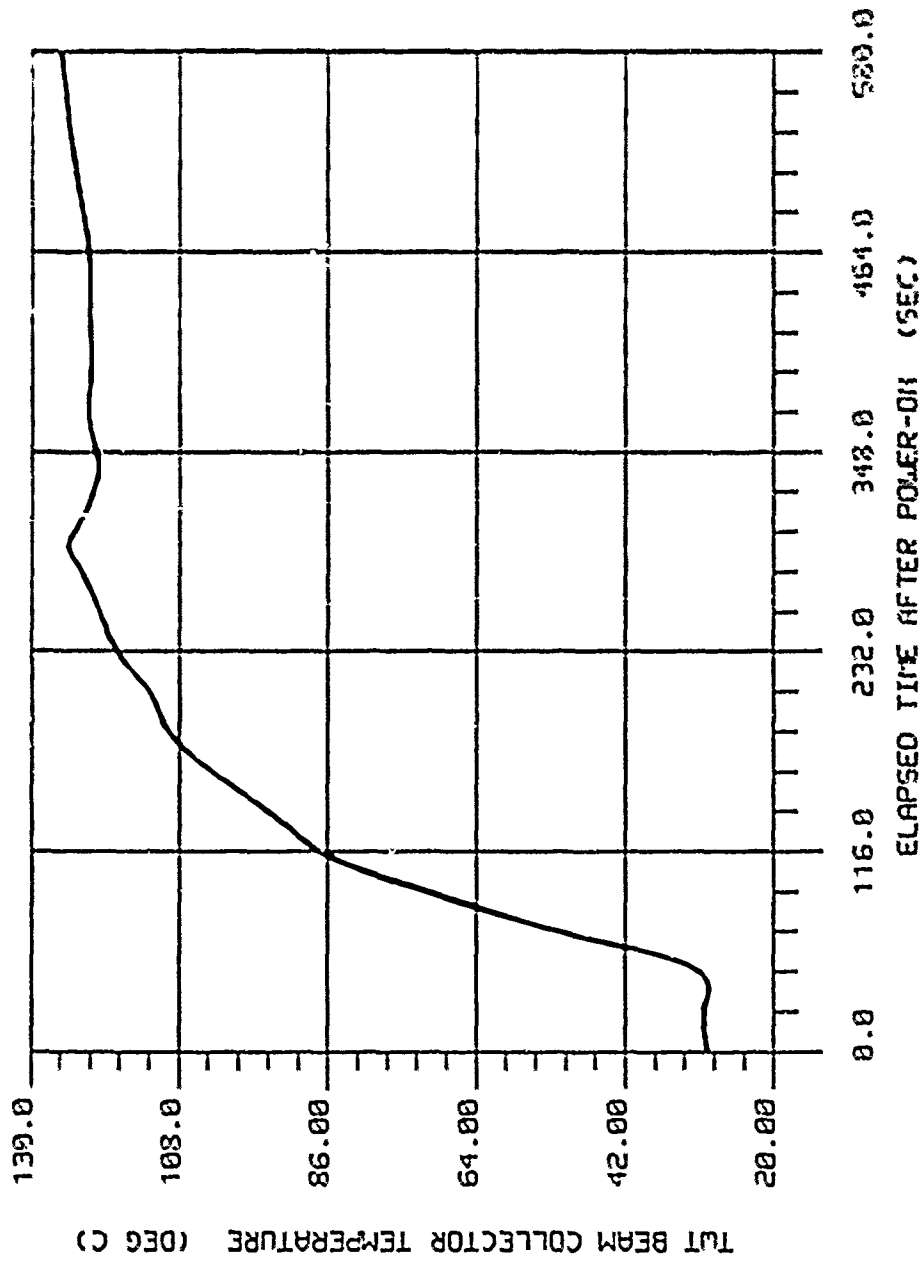ELAPSED TIME AFTER POWER-ON (SEC)

FIGURE 5

RF window, therefore, it was assumed that the system's heat sink temperature followed this time-amplitude curve. A number of data points were inserted into the input file to represent this curve. The curve was then referenced by the sink temperature data group in the NISA input file to give temperature and heat source values at any time.

Results

NISA's transient heat transfer program was executed in time steps of ten seconds over a span of 580 seconds. Temperature contours for 50 and 100 watt heat sources are shown in Figures 6a and 6b (all temperature units are given in degrees C). These plots show the system's thermal state at the conclusion of the run (580 seconds). It is apparent that the widths of the temperature bands through the beryllia are wider than through the other materials. This is because of beryllia's much higher thermal conductivity. Figures 7a and 7b, obtained through NISA's post processor, are time vs. temperature curves at four nodes in the model for heat dissipation rates of 50 and 100 watts respectively. Temperature values at nodes 1, 65 and 481 were plotted because these are the nodes of maximum temperature for the copper, beryllia and monel, respectively. In all cases, the temperature of the model reaches a maximum at approximately 290 seconds and remains relatively constant for the duration of the run. Node 1 is the node of greatest temperature change from the heat sink since it is one of the nodes where heat is being generated. Nodal temperatures decrease with increasing distance from the heat source.

17

The results of these heat transfer analyses have shown that at any time during the TWT's operation, the temperature distribution throughout the RF window is in the radial direction and does not vary in the vertical direction.

Temperature Distribution – 50 Watts

ISOTHERM CONTOURS
TRANSIENT HEAT

VIEW : 1.26E+02
RANGE : 2.74E+02

274.5
257.9
241.4
224.8
208.3
191.8
175.2
158.7
142.1
125.6

EMRC-NISA/DISPLAY

RX= 0
RY= 0
RZ= 0

FIGURE 6a

19

Temperature Distribution–100 Watts

ISOTHERM CONTOURS
TRANSIENT HEAT
VIEW: 1.26E+02
RANGE: 4.23E+02

9	423.3
8	390.3
7	357.2
6	324.1
5	291.0
4	257.9
3	224.8
2	191.8
1	158.7
	125.6
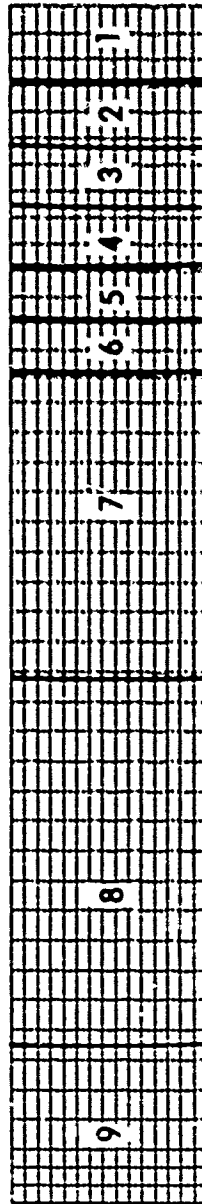
EMRC-NISA/DISPLAY

Y   RX= 0
         RY= 0
Z   X   RZ= 0

FIGURE   6b

20

Time vs Temperature Curves 50 Watts

FIGURE 7a

21
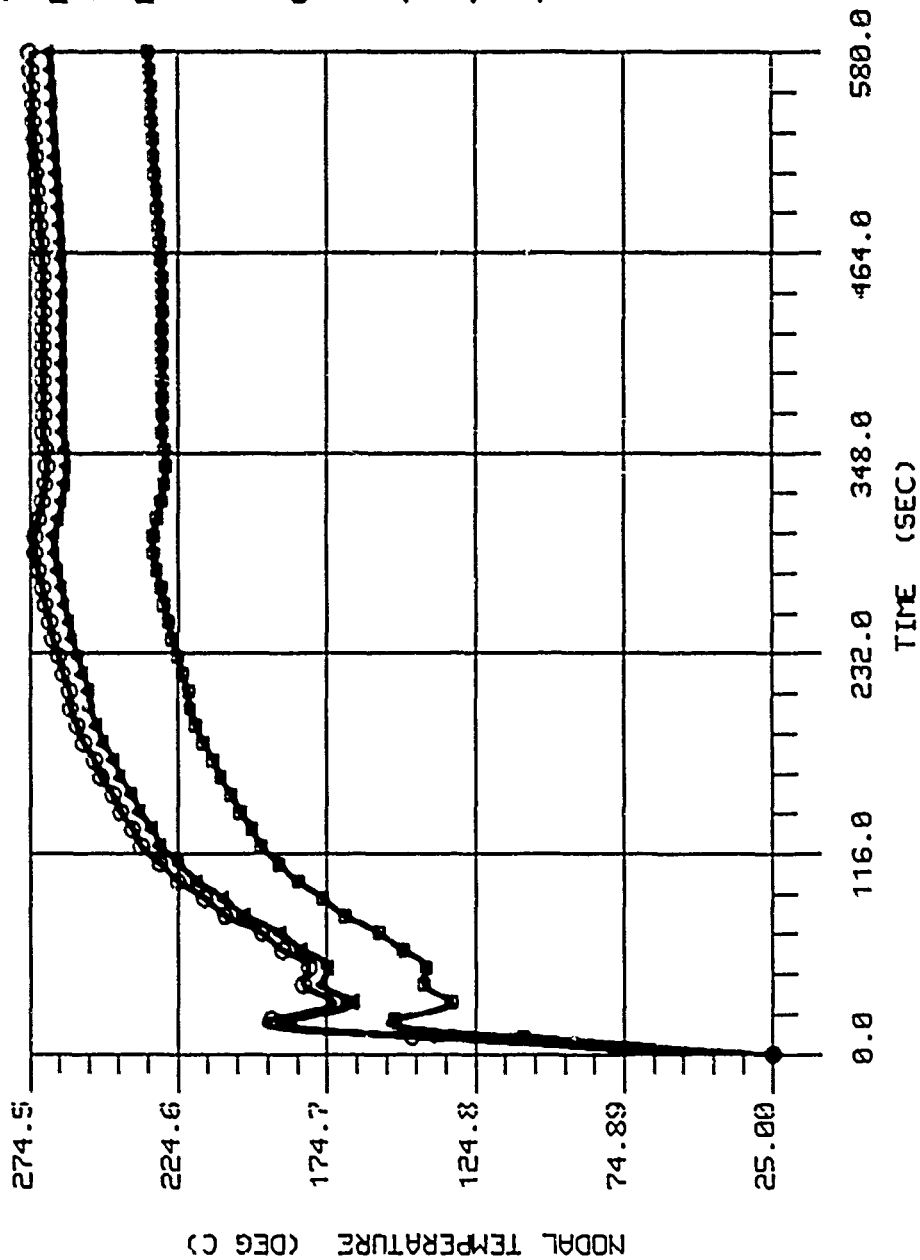
Time vs Temperature Curves 100 Watts
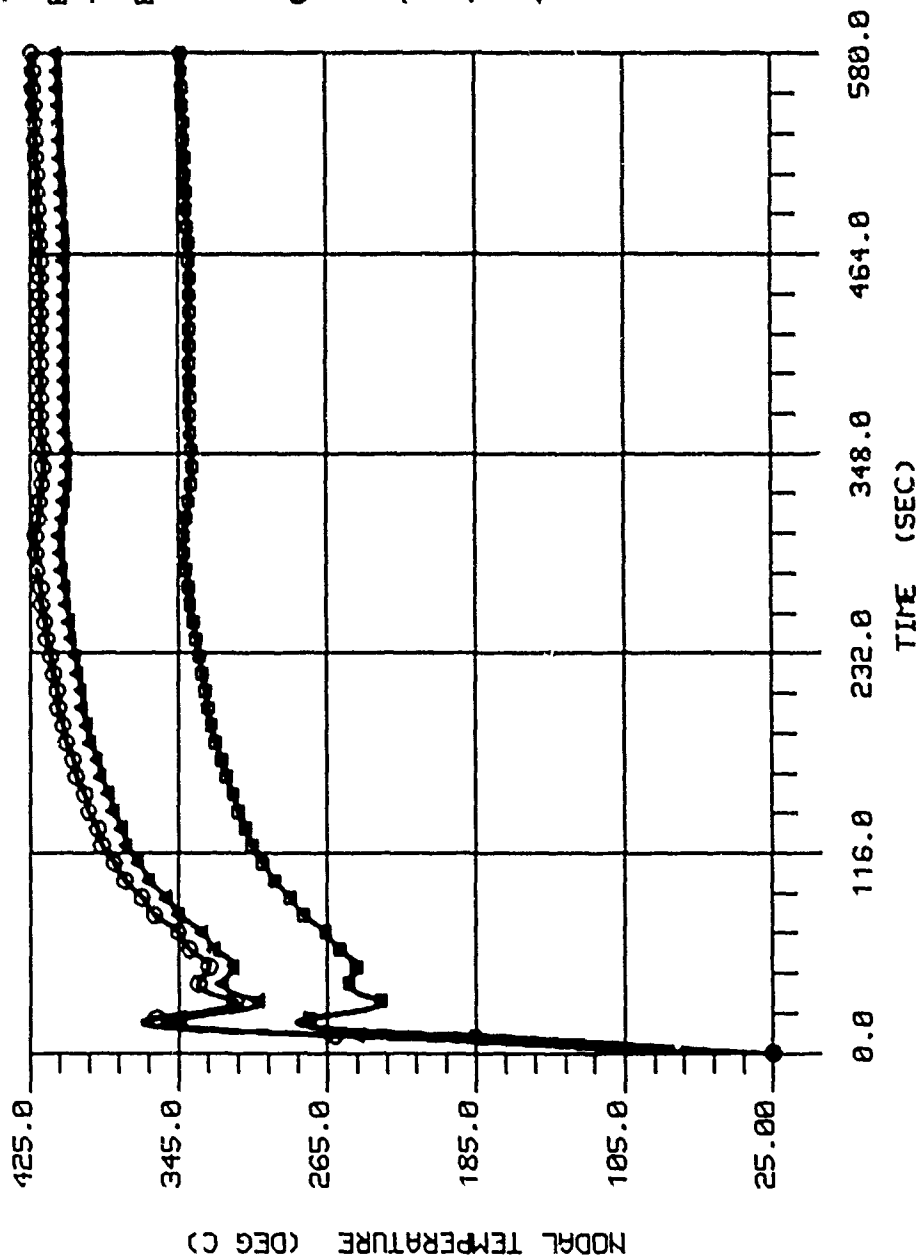
FIGURE 7b

4.0 THERMAL STRESS ANALYSES

Thermal stresses are stresses arising from temperature variations within a material. When a material is subjected to a temperature gradient, the various fibers tend to expand different amounts. This expansion induces tensile and compressive stresses throughout, if the material is physically constrained. When these stresses exceed the yield strength, deformation and/or failure will occur.

The results of NISA's transient heat transfer analysis gave temperatures at each node for a given heat source. The resulting output file was saved at the time step where maximum temperature occurs for each source and used as a thermal loading condition into NISA's nonlinear static stress module. This time step was chosen at the conclusion of each run (580 seconds) which also corresponded to the steady state condition. These nonlinear stress analyses take into account the behavior of a ductile material's stress-strain curve beyond its yield point. Data points containing stress and corresponding strain values for both copper and monel beyond their respective yield points were inserted into the input file. Copper's stress-strain curve beyond its yield point is shown in Figure 12. The same time-amplitude curve used to represent the sink temperature in the transient heat transfer analyses was used to represent the temperature loading in these nonlinear stress analyses.

A series of thermal stress analyses were performed on the RF output window. First, stress analyses of the window were made when the entire

23

system was assigned a finite temperature (zero heat generation). This was done to determine if cracking of the beryllia could possibly occur when the TWT was in the power off condition and subject to extremely cold ambient temperatures. A nonlinear static stress analysis was made with the entire temperature of the system being dropped to $-150^{\circ}C$ (approximately $-83^{\circ}F$). The results showed the maximum principal stress to be 84.86N/sq mm and the minimum principal stress to be -192.33N/sq mm. Since neither of these values approach the tensile or compressive stress of beryllia (159 and -130,000N/sq mm, respectively), the beryllia will not crack under this condition.

Next, stress analyses were made using the heat transfer results for heat dissipation rates ranging from 20 to 120 watts. These results allowed several plots to be developed relating thermal stresses to elapsed time after power up of the system. Because of a lack of information regarding stress-free temperature for these materials, it was assumed that a state of zero stress existed at $25^{\circ}C$ (approximately room temperature). Stresses at each node were dependent upon the difference between the temperature at that node and this stress-free temperature. The results do not consider the residual stresses that exist prior to power up. Residual stresses, in general, are caused by prior thermal cycling, manufacturing processes, creep, etc. Since copper and monel were assumed to behave as ductile materials, and beryllia a brittle material, different methods of determining the possibility of failure had to be employed.

Beryllia

Failure of brittle materials occurs due to a peak load. These materials do not fail due to accumulation of fatigue, as do ductile materials. To predict brittle fracture, the maximum normal stress theory was used. This stipulates that fracture in a brittle material will occur whenever the maximum principal stress at a point, if it is in tension, is equal to or greater than the tensile strength of the material. Similarly, if the specimen is in compression, failure will occur if the algebraic minimum principal stress at a point is equal to or more negative than the material's compressive strength (7). Principal stresses are normal stresses associated with axes on whose normal planes there exist extreme normal stress and zero shear stress. It is generally the case, and this case is no exception, that materials have greater strength in compression than in tension. Beryllia has a tensile strength of 159 N/sq mm and a compressive strength of 130,000 N/sq mm. (Appendix A contains properties for all materials used in this study.)

Figures 8a and 8b are plots of maximum principal stress (N/sq mm) through the beryllia with 50 and 100 watts of heat being dissipated through the window, respectively. All positive stress values indicate tension, while all negative stress values indicate compression. These contours demonstrate the increased stress levels associated with increased heat dissipation. Higher heat dissipation rates induce more positive tensile stresses and more negative compressive stresses. Figures 9a and 9b are curves of time vs. maximum principal stresses at node 142 in the beryllia

25

at 50 and 100 watts heat dissipation. Node 142 is located at the beryllia-monel interface and is the node of maximum principal stress (maximum tension) for the beryllia. Tensile stresses are greatest at the nodes near the outer diameter of the beryllia because as the system is heated, the monel undergoes greater expansion than does the beryllia (this is because monel has a greater coefficient of thermal expansion than beryllia), causing the beryllia to be in tension. When heat is being dissipated through the window at a rate of 20 watts, a maximum principal stress of 156.5N/sq mm was calculated. Since this value approaches beryllia's tensile strength of $159N/mm^2$, cracking of the beryllia can be expected to occur for heat dissipation rates above 20 watts.

Stress Distribution – BeO 50 Watts

226.9

199.9

172.9

145.9

118.9

91.95

64.95

37.95

10.96

-16.03

EMPC-NISA DISPLAY

PX= 0
PY= 0
PZ= 0

FIGURE 8a

27

Stress Distribution-BeO 100 Watts

STRESS CONTOURS
S1 PRINCPL STRESS
VIEW: -4.25E+01
RANGE: 3.44E+02

9	391.4
8	342.8
7	294.1
6	245.5
5	196.9
4	148.2
3	99.59
2	50.95
1	2.32
	46.31

EMRC-NISA/DISPLAY

RX= 0
RY= 0
RZ= 0

FIGURE   8b

28
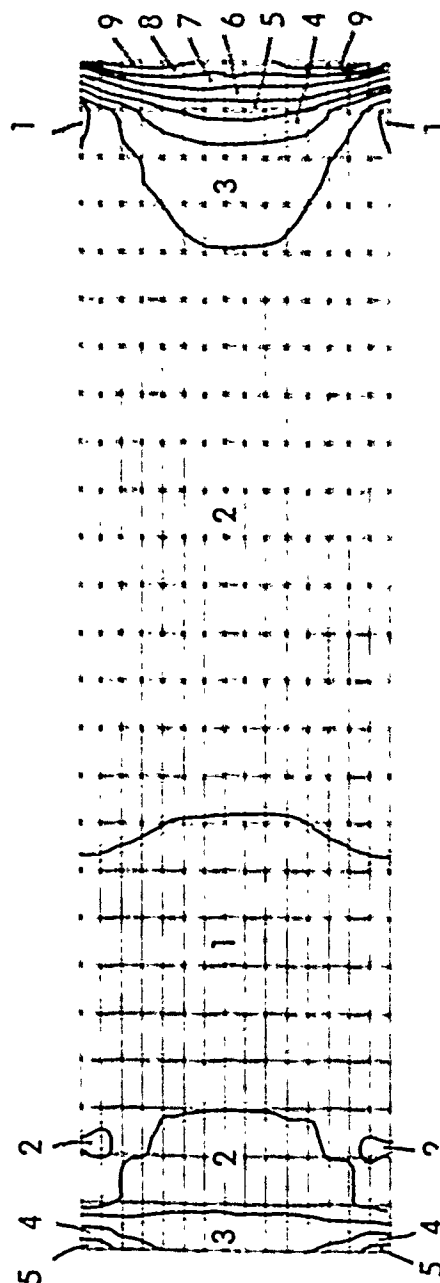
Time vs Stress Curve-Node 142   50 Watts

TIME - HISTORIES

SIP   : 3.33E+01
RANGE : 2.27E+02
TIME : 2.90E+01
RANGE : 5.80E+02

S1 (MAX) PRINCIPAL STRESS (N/sq mm)

230.0
190.0
150.0
110.0
70.00
30.00

29.00   139.2   249.4   359.6   469.8   588.0

TIME (SEC)
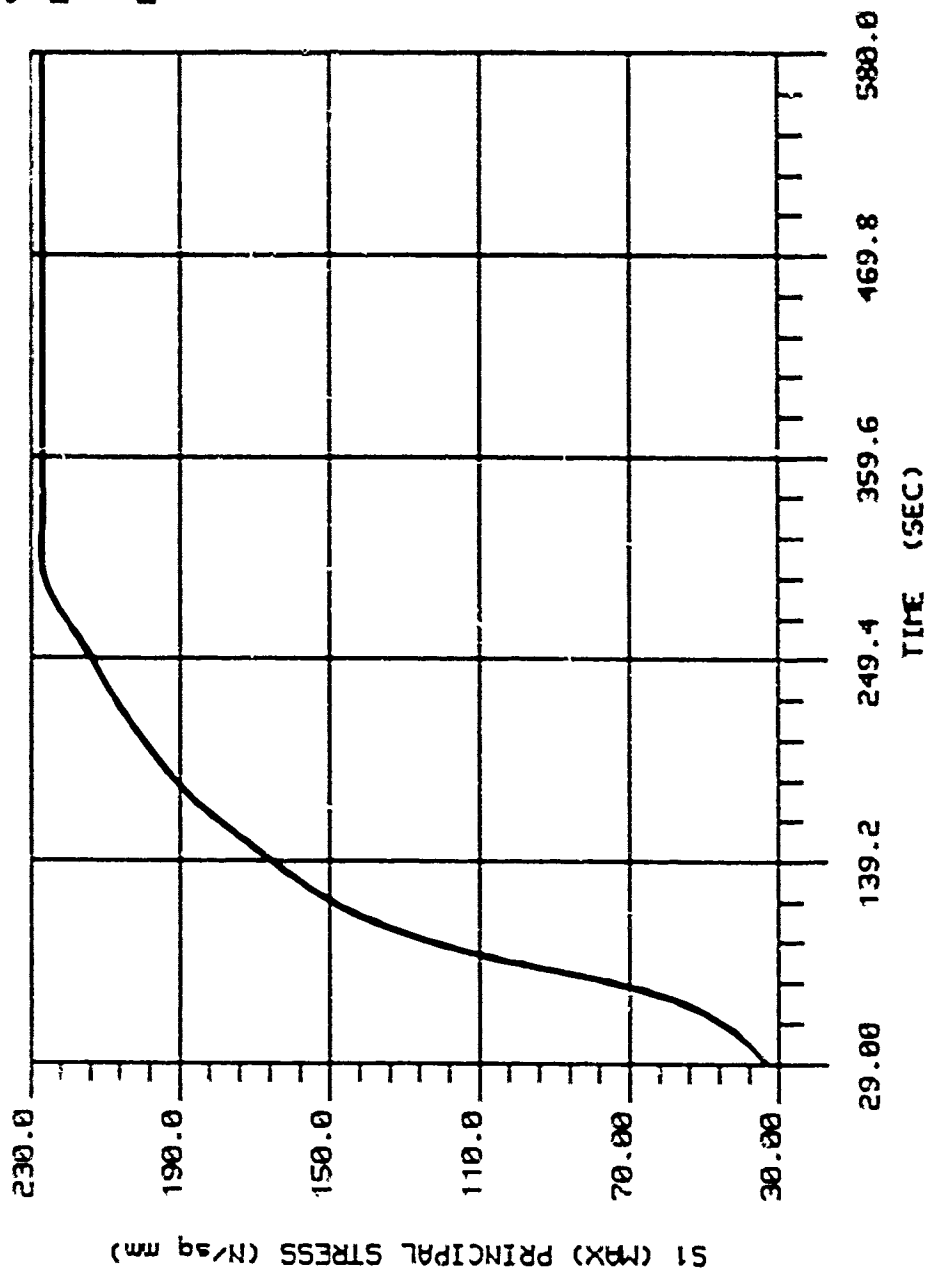
FIGURE   9a

Time vs Stress Curve–Node 142   100 Watts

TIME - HISTORIES

S1P :	7.24E+01
RANGE :	3.91E+02
TIME :	2.59C+01
RANGE :	5.80E+02

FIGURE   9b
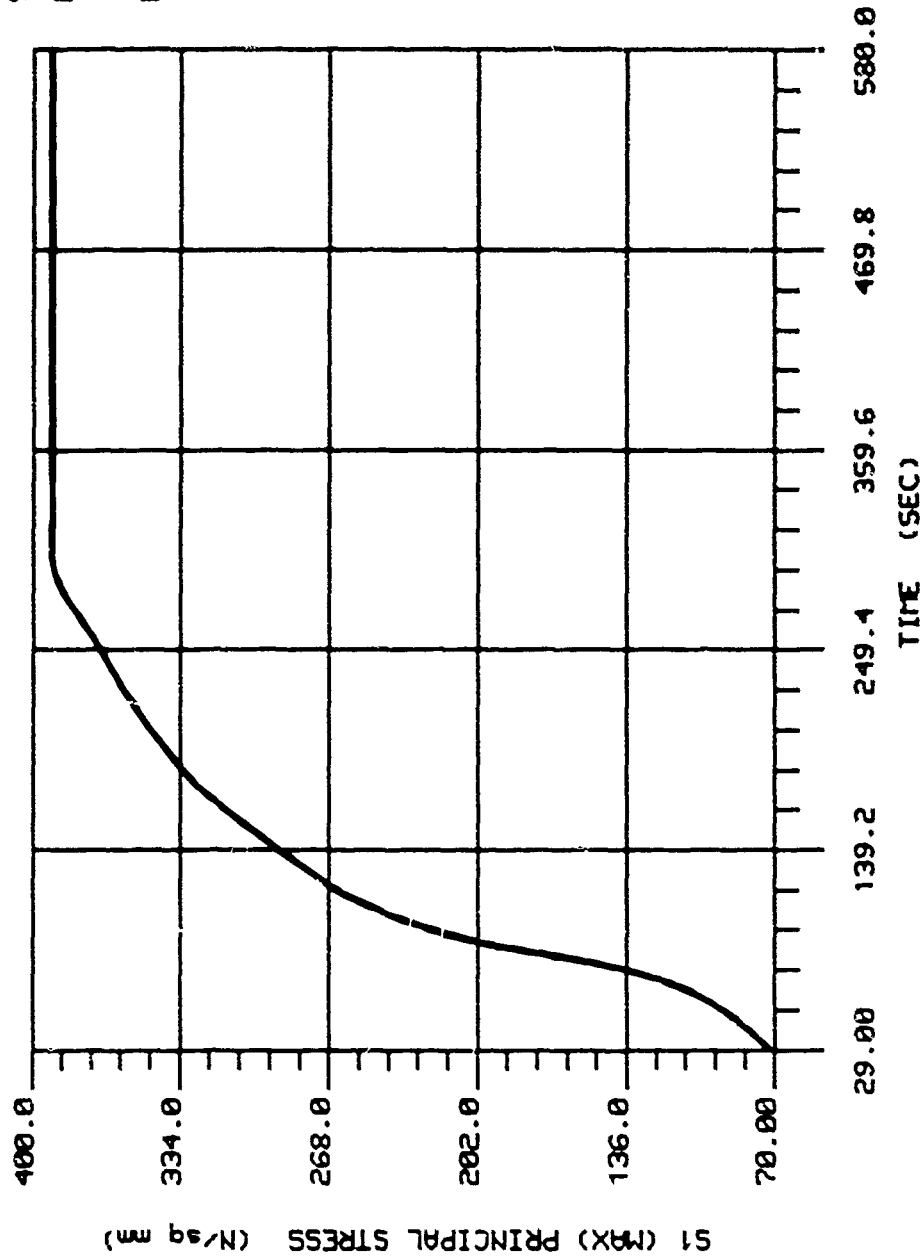
S1 (MAX) PRINCIPAL STRESS (N/sq mm)

TIME (SEC)

Copper

In order to predict the life of the copper portion of the RF window, the effect of fatigue due to power cycling was studied. The system experiences one power cycle when it goes from its initial, or stress-free temperature, to its power up temperature, then back to its original state. If, when the system is powered up, the stresses through the copper exceed its yield stress, the copper will experience a certain amount of strain. After the system is returned to its original thermal state, only the elastic strain is recovered. The strain that remains within the material, the plastic strain, accumulates with every power cycle. Therefore, after a certain number of power cycles, the strain will reach a high enough value to cause the copper to fail.

When determining the total strain, the following procedure is used. First, Von-Mises stresses in the copper are determined. The Von-Mises stress is a combined stress value that is widely accepted in predicting failure of ductile materials. Von-Mises stresses through the copper were calculated for different values of heat dissipation. Figures 10a and 10b are contour plots of Von-Mises stresses in the copper for 50 and 100 watts of heat dissipation. As was the case with beryllia, the stress levels increased with increased heat dissipation through the window. The Von-Mises stress is a maximum at nodes 4 and 64, the lower and upper corners of the copper-beryllia interface, respectively. Since the distribution is symmetric about the center of the model, these stress values are identical and only the data for node 4 was taken into account. The Von-Mises

31

Stress Distribution - Cu 50 Watts

STRESS CONTOURS
VON-MISES STRESS
VIEW : 4.74E+01
RANGE : 5.46E+01

54.64
53.84
53.03
52.22
51.41
50.60
49.80
48.99
48.18
47.37

EMPC-HISA-DISPLAY

RX= 0
RY= 0
RZ= 0

FIGURE 10a

Stress Distribution--Cu 100 Watts

STRESS   CONTOURS
VON-MISES STRESS
VIEW: 5.24E+01
RANGE: 6.32E+01

9	66.46
8	65.12
7	63.77
6	62.42
5	61.08
4	59.73
3	58.38
2	57.04
1	55.69
	54.34

EMRC-NISA/DISPLAY

Y   RX=   0
           RY=   0
Z   X   RZ=   0

FIGURE   10b

33

Time vs Stress Curve–Node 4 50 Watts

TIME - HISTORIES

SO2 : 4.45E+01
RANGE : 5.47E+01
TIME : 2.90E+01
RANGE : 5.80E+02

TIME (SEC)

VON-MISES STRESS (N/sq mm)

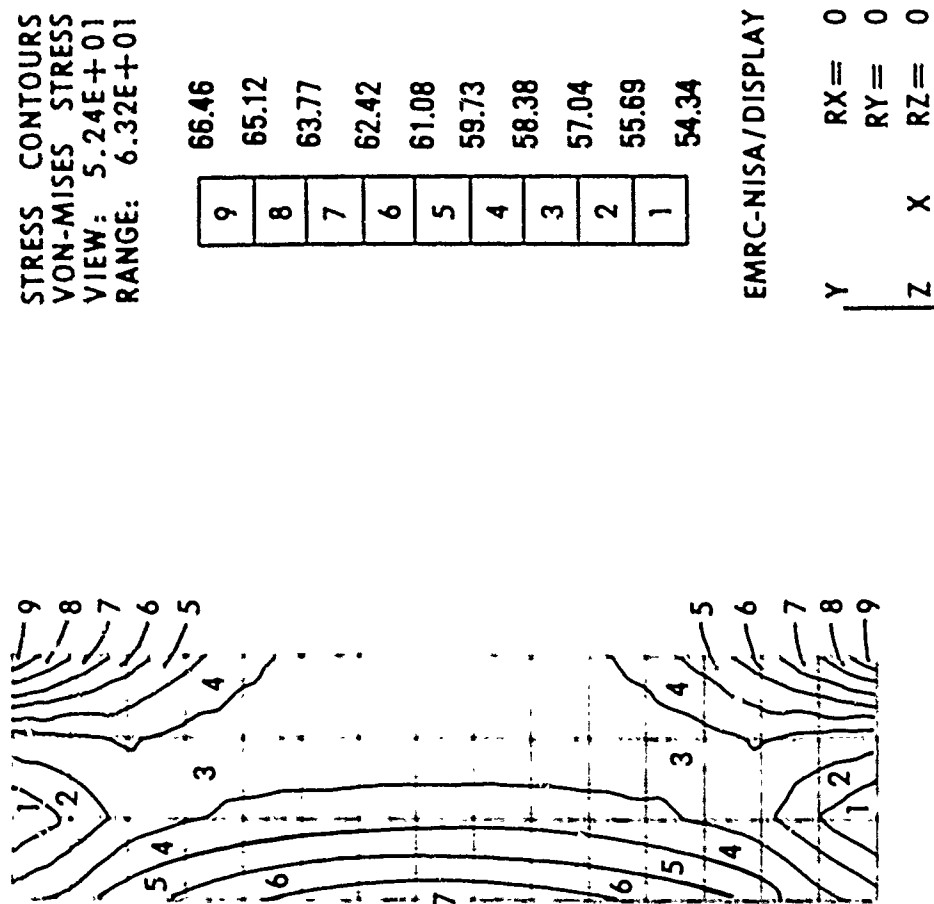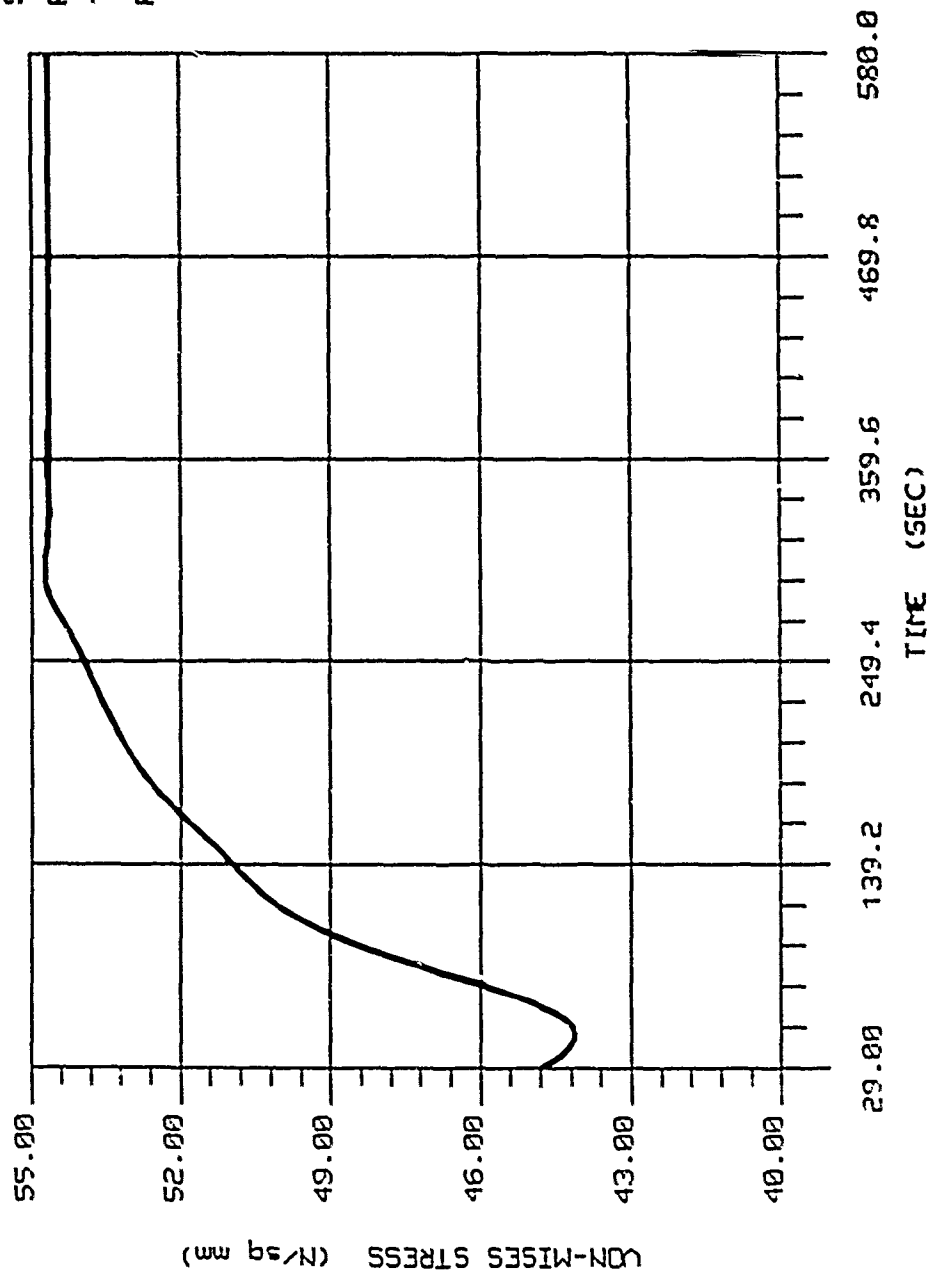## FIGURE 11a

Time vs Stress Curve-Node 4   100 Watts

TIME - HISTORIES
S02   : 4.63E+01
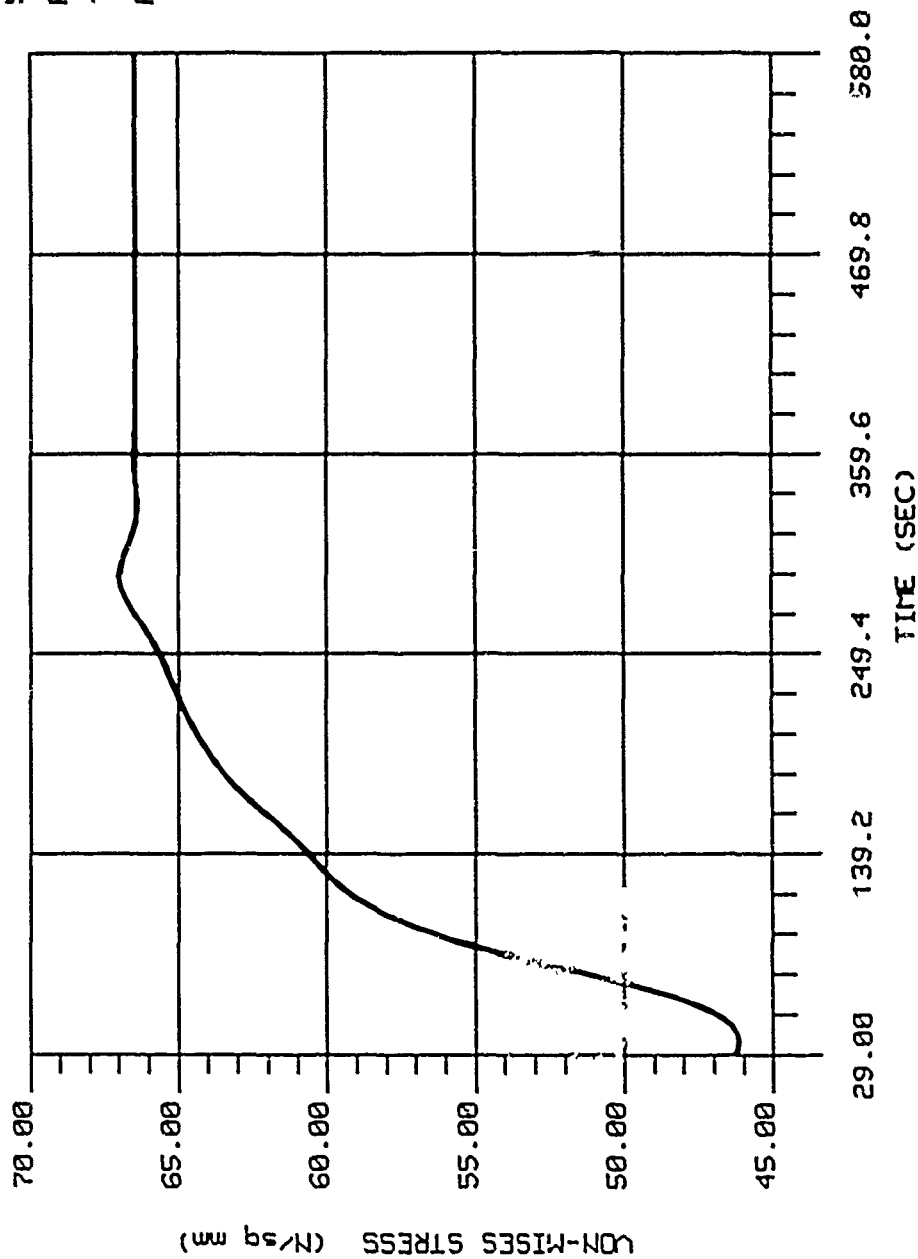RANGE : 6.70E+01
TIME : 2.90E+01
RANGE : 5.80E+02

FIGURE   11b

35

stresses are plotted in Figures 11a and 11b against elapsed time after power up at node 4. This curve demonstrates the increase in the Von-Mises stress up until approximately 290 seconds, when the TWT operating temperature reaches a maximum (see TWT operating profile in Figure 5). After this time, the stresses increase only slightly as time is increased.

The total strain is then obtained for a given stress from the stress-strain curve for copper shown in Figure 12. This total strain value is translated into number of cycles to failure using the Manson-Coffin relation for a specific material. The Manson Coffin model, along with the parameter values for copper, is shown in Figure 13. These values were inserted into the Manson-Coffin model and a plot, shown in Figure 14 was generated. This plot contains two lines and one curve. The lines represent the elastic and plastic components and the curve represents the sum of these two components. To obtain the number of cycles to failure for a given strain, the total strain value at node 4 is plotted onto the curve and the number of cycles to failure is determined. The chart below lists maximum Von-Mises stresses (node 4), strains, and power cycles to failure for different values of heat dissipation rates.

HEAT (WATTS)	STRESS (N/sq mm)	STRAIN	CYCLES
20	49.18	.0054	9000
50	56.64	.007	1450
80	59.62	.011	950
90	61.49	.0118	800
100	63.17	.0125	700
120	65.96	.0145	500

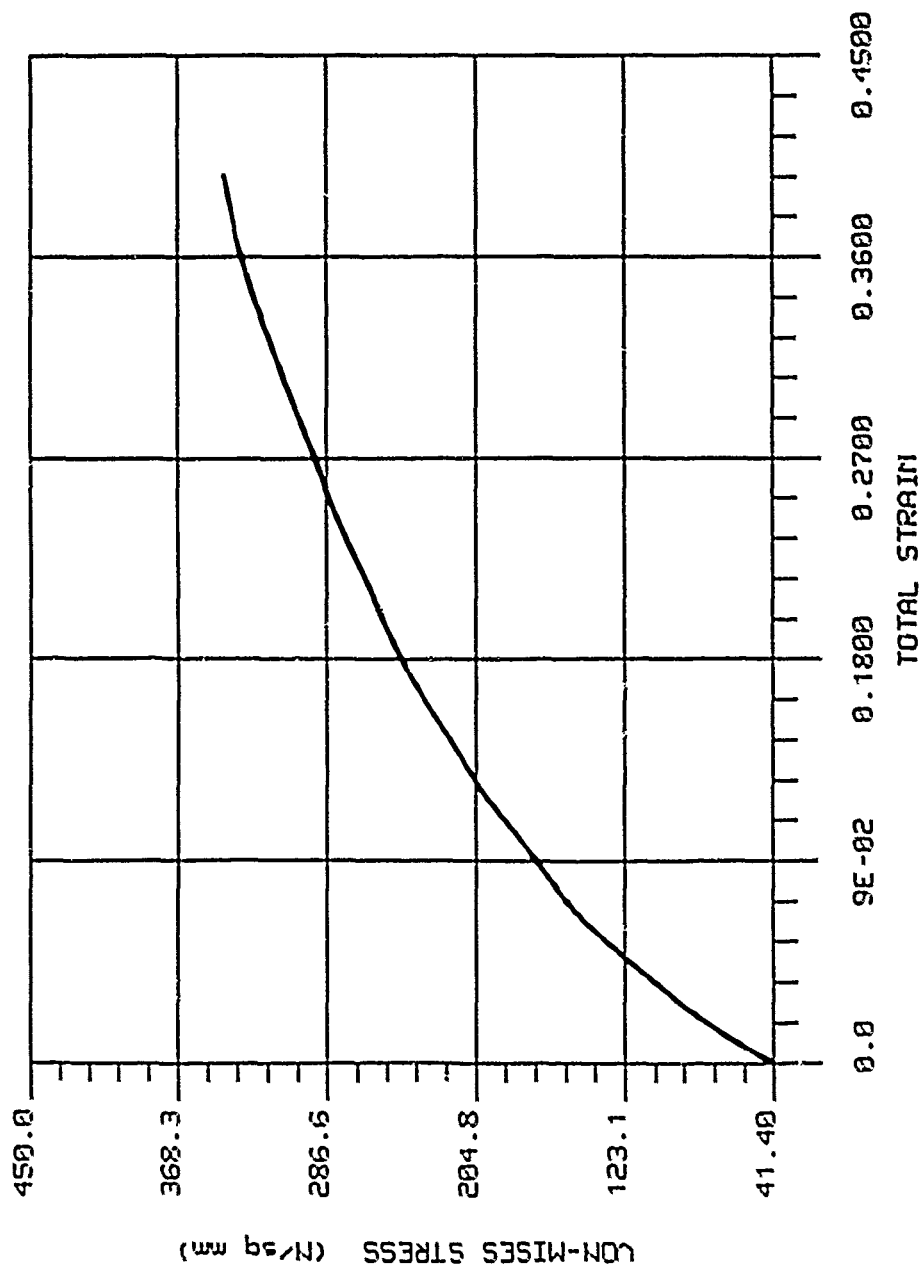Stress–Strain Curve For Copper (Above Yield Point)

FIGURE 12

Manson–Coffin Model

$$\frac{\Delta \epsilon}{2} = \underbrace{\frac{\sigma_f}{E} (2N_f)^b}_{\substack{\text{ELASTIC} \\ \text{STRAIN}}} + \underbrace{\epsilon_f (2N_f)^c}_{\substack{\text{PLASTIC} \\ \text{STRAIN}}}$$

PARAMETER	COPPER
σ_f	345 N/sq mm
ϵ_f	.3
E	1.25 E6 N/sq mm
b	-.05
c	-.6

σ_f : FATIGUE STRENGTH COEFFICIENT
ϵ_f : FATIGUE DUCTILITY COEFFICIENT
E : MODULUS OF ELASTICITY
b : FATIGUE STRENGTH EXPONENT
c : FATIGUE DUCTILITY EXPONENT

FIGURE 13

Manson–Coffin Curve For Copper

FIGURE 14

39
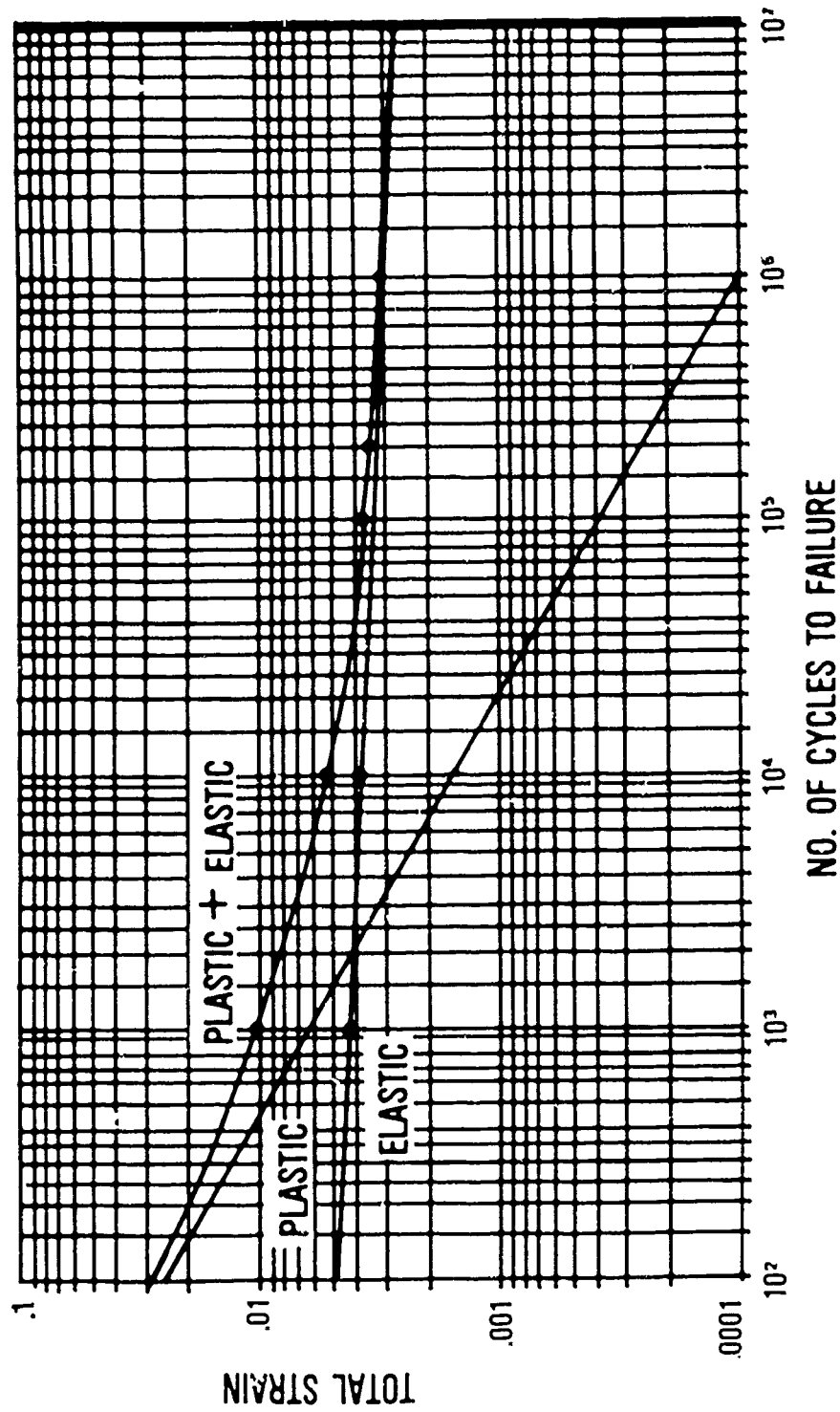
A plot of heat dissipation through the window (normal scale) vs. number of power cycles to failure (log scale) for the copper is shown in Figure 15. This plot indicates that an increased heat input will cause a decrease in the number of cycles to failure, indicating a less reliable system. By using this graph for a given heat input, a number of power cycles to failure can be determined.

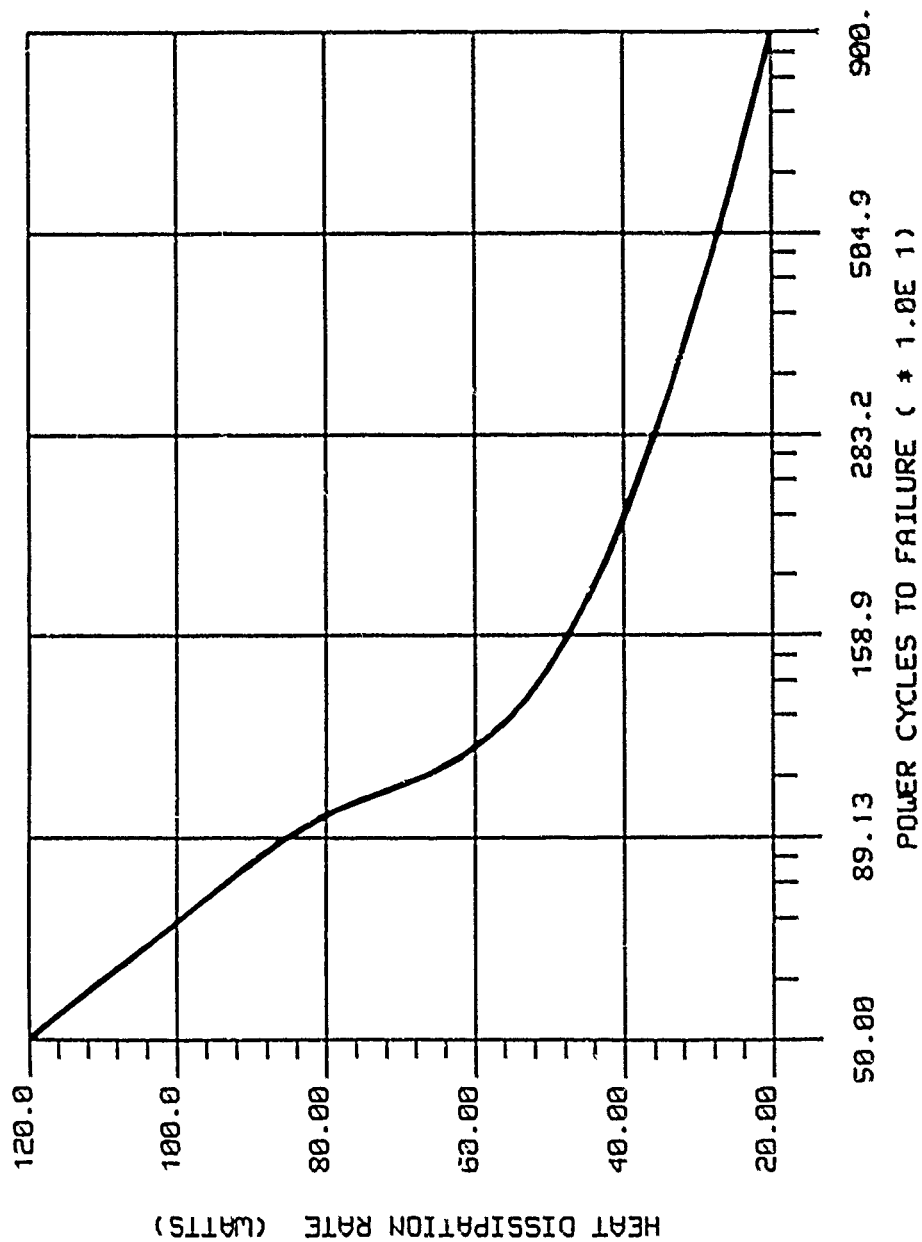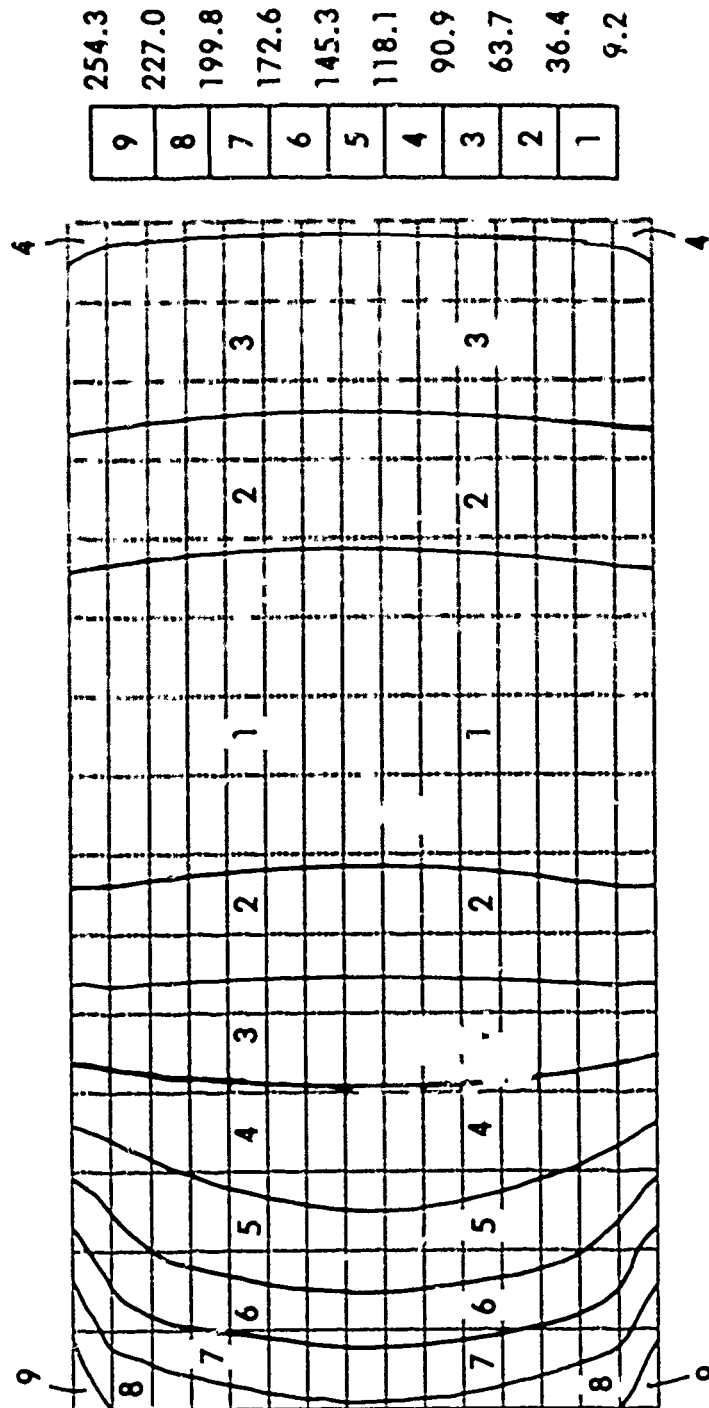# Cycles To Failure vs Heat Dissipation –Copper

FIGURE 15

Monel

Like copper, monel behaves in a ductile manner. Von-Mises stresses were calculated and their contours are plotted in Figures 16a and 16b for heat sources of 50 and 100 watts, respectively. These contour shapes remain approximately the same for all cases with the larger stress magnitudes occurring for larger heat sources.

Time vs. stress curves were then plotted for 50 and 100 watt heat sources at node 481 (Figures 17a and 17b). The largest Von-Mises stresses through the monel occurred at this node which is located at the lower corner of the beryllia-monel interface.

Monel's yield stress of 758N/sq mm was not exceeded for any of the nonlinear static runs that were performed (up to 120 watts). Therefore, this portion of the window is not expected to contribute to the RF window's failure.

Stress Distribution – Monel   50 Watts

STRESS   CONTOURS
VON-MISES   STRESS
VIEW: 9.19E+00
RANGE: 2.54E+02

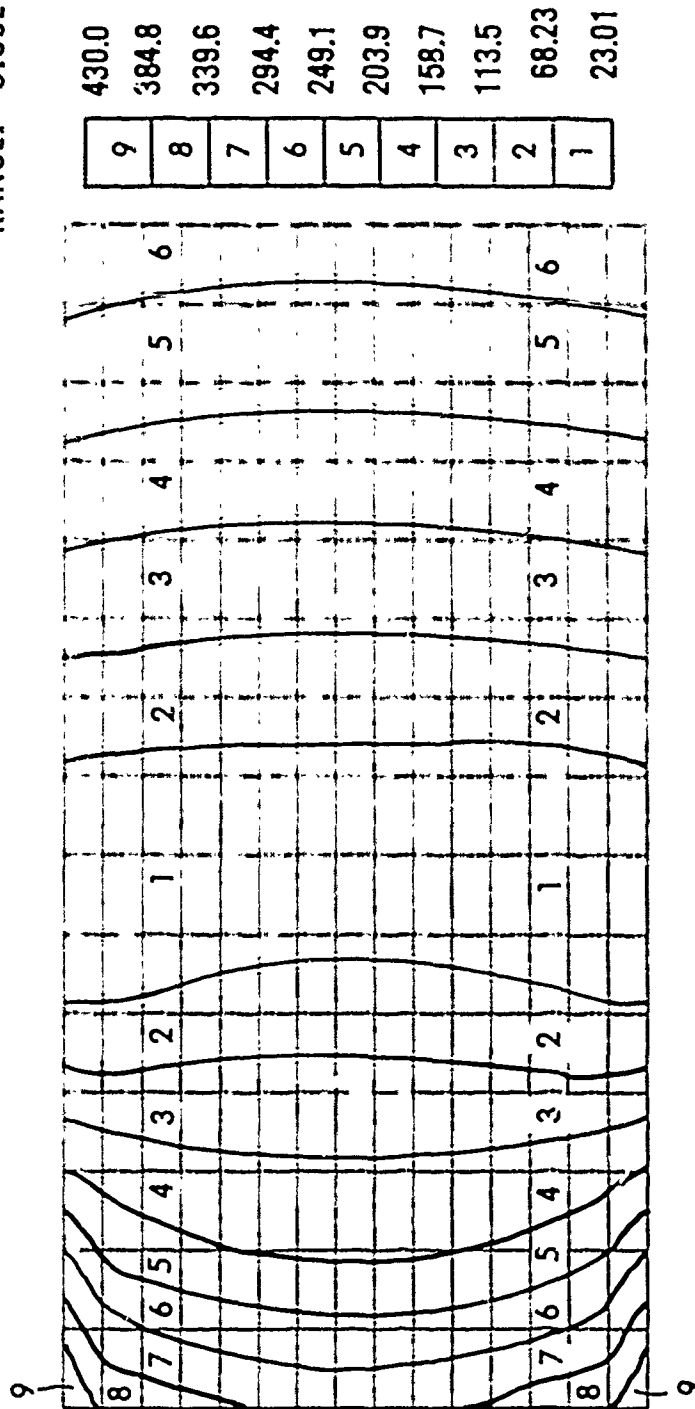|	
9	254.3
8	227.0
7	199.8
6	172.6
5	145.3
4	118.1
3	90.9
2	63.7
1	36.4
1	9.2

EMRC-NISA/DISPLAY

RX= 0
RY= 0
RZ= 0

Y

Z   X

FIGURE 16a

43

Stress Distribution – Monel 100 Watts

STRESS CONTOURS
VON-MISES STRESS
VIEW: 2.13E+01
RANGE: 3.80E+02

9	430.0
8	384.8
7	339.6
6	294.4
5	249.1
4	203.9
3	158.7
2	113.5
2	68.23
1	23.01

EMRC-NISA/DISPLAY

RX= 0
RY= 0
RZ= 0

FIGURE 16b

44

Time vs Stress Curve – Node 481 100 Watts

TIME - HISTORIES

SG2   : 7.76E+01
RANGE : 4.30E+02
TIME   : 2.90E+01
RANGE : 5.89E+02

VON-MISES STRESS   (N/sq mm)

435.0
363.0
291.0
219.0
147.0
75.00

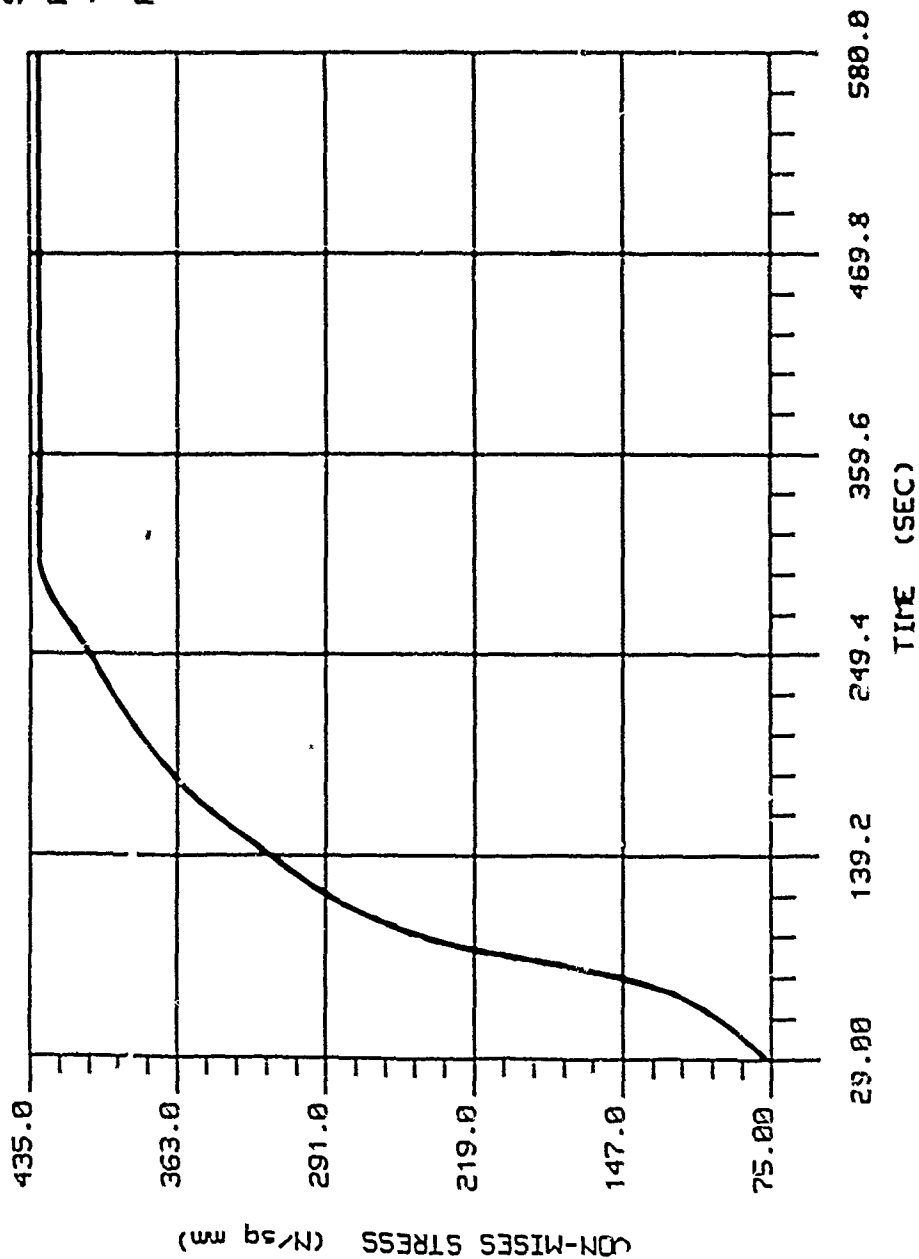29.00   139.2   249.4   359.6   469.8   580.0

TIME (SEC)

FIGURE 17

45

5.0 CONCLUSIONS

Microwave tube reliability is strongly dependent on three factors. First, defects introduced during the manufacturing process adversely affect reliability. Producibility problems, poor workmanship and lack of process control are major contributors to manufacturing defects. Secondly, tube reliability is heavily dependent upon operating procedures and handling. Finally, adequate design margin must exist between the operating point and the ultimate design capability of the tube in order to have reliable operation.

At the onset of this study, it was assumed that neither manufacturing processes nor handling procedure played a part in the failure of this window. It was the purpose of this study to investigate the impact of increased operating temperature on its structural integrity.

The two most significant conclusions made based on the results of these analyses were:

- At heat dissipation rates greater than 20 watts, cracking of the beryllia would begin to occur.

- Depen . . . . mount of heat being dissipated through the system, the copper port on of the window could be expected to survive anywhere between 500 and 9000 power cycles.

Some other conclusions that can be made from these results are:

- Cracking of the beryllia would occur in tension, there was no evidence found that would predict compressive failure.

- A stress analysis of the system in the power off condition subject to an extremely cold ambient temperature (-150°C) indicated that the beryllia would not fail under this extreme.

- Stresses through the monel portion of the window did not approach its yield stress for any of the analyses made. Therefore, this region will not contribute to the window's failure.

The results of this study have demonstrated that finite element analysis is a valuable tool that can be used to predict structural reliability of this RF window. Lack of sufficient TWT data did not permit a conclusion to be made on whether inadequate design or operation beyond design limits had caused the window to fail. It should be noted that this study was limited to an output window of this size, composition and operating environment.

Finite element analysis can prove to be a valuable tool in advancing TWT technology by aiding in the design of future TWT components. Up-front structural reliability assessments can be made on a component before production actually begins to insure that it can withstand the conditions it was designed for. Finite element analysis can also be used as an analysis

tool for identifying design flaws in previously failed tubes and assist in the diagnostics associated with forensic analysis of these tubes.

6.0 REFERENCES

1. Askeland, D. R., "The Science and Engineering of Materials", Wadsworth, Inc., 1984.

2. Hughes Aircraft Company, "Hughes TWT and TWTA Handbook".

3. Hughes Aircraft Company, "Reliability Design Criteria For High Power Tubes", February,1989, RADC-TR-88-304, Vol. 1, pp. 2-116 - 2-118.

4. Incropera, F. P. and DeWitt, D. P., "Fundamentals of Heat and Mass Transfer", John Wiley & Sons, Inc., 1985.

5. Muehe, C. E., "Thermal Cracking of Waveguide Windows", Massachusetts Institute of Technology, Lincoln Laboratory, February, 1966.

6. Sandor, B. I., "Fundamentals of Cyclic Stress and Strain", The University of Wisconsin Press, 1972.

7. Shames, I. H., "Introduction to Solid Mechanics", Prentice-Hall, Inc., 1975, pp. 371-384.

8. Staprans, A., McCure, E. W., and Ruetz, J. A., "High Power Linear Beam Tubes", Proceedings of the IEEE, Vol. 61, No. 3, March 1973.

APPENDIX A

MATERIAL PROPERTIES

COPPER
Material ID=1
E=1.24 E+05
NU=.34
ALPHA=17.6 E-06
k=.389 @ -73 DEG C
.401   @ 27   "   "
.409   @ 127   "   "
.424   @ 327   "   "
Y= 41.4
C= 385
DENS= 8.47 E-06

BERYLLIA
Material ID=2
E=3.25 E+05
NU= .23
ALPHA=8.0 E-06
TENS. ST.=159.0
COMP. ST.=1.3E+05
k=.272 @ 27   DEG C
  .196 @ 127   "   "
  .111 @ 327   "   "
  .07 @ 527   "   "
DENS= 3.0E-06

MONEL K-500
Material ID=3
E=1.79 E+05
NU=.32
ALPHA=13.68 E-06
Y=758.5
k=.01745
C= 418.7
DENS= 8.47 E-06

ELASTIC
Material ID=4
E=2.76 E+04
NU=.4
ALPHA=5.0 E-04

SYMBOL AND DEFINITION	UNITS
E:	Modulus of Elasticity	N/sq mm
NU:	Poissons Ratio	Dimensionless
ALPHA:	Coefficient of Thermal Expansion	1/DEG C
Y:	Yield Strength	N/sq mm
TENS ST:	Tensile Strength	N/sq mm
COMP ST:	Compressive Strength	N/sq mm
k:	Thermal Conductivity	Watts/mm C
C:	Specific Heat	Joules/kg C
DENS:	Mass Density	kg/cubic mm

MISSION
of
Rome Air Development Center

RADC plans and executes research, development, test and selected acquisition programs in support of Command, Control, Communications and Intelligence (C³I) activities. Technical and engineering support within areas of competence is provided to ESD Program Offices (POs) and other ESD elements to perform effective acquisition of C³I systems. The areas of technical competence include communications, command and control, battle management information processing, surveillance sensors, intelligence data collection and handling, solid state sciences, electromagnetics, and propagation, and electronic reliability/maintainability and compatibility.